International Journal of Recent Technology and Engineering (IJRTE)
ISSN: 2277-3878 (Online), Volume-8 Issue-4, November 2019

Human Driver Interaction with Self-Balancing Vehicles' Dynamics

Paolo Righettini, Vittorio Lorenzi, Bruno Zappa, Roberto Strada

Abstract*: This paper deals with a research activity concerning two-wheel self-balancing vehicles, with particular reference to the interaction between the driver and the vehicle's dynamics. The usefulness and the flexibility of this kind of vehicle make it a very interesting device for smart mobility. In particular, a dynamical model of a two wheeled self-balancing vehicle and of his driver is presented here. It consists of a Multibody model of a real vehicle, designed and built in the Mechatronics and Mechanical Systems Dynamics lab. of our University, and of a driver model with 3 driven joints. The overall 3D model developed allows simulating the interaction between human (driver) and machine (vehicle), taking into consideration also the coupling between longitudinal motion and turn. The vehicle's control system has been synthesized using the pole placement approach, starting from a simplified 2 dof planar model of the vehicle, considering the driver fixed with vehicle chassis. Through proper linearization, a state space description has been obtained and used to tune pole position, not only for stability but also for optimal response. Through co-simulation between the controller (modelled in Matlab-Simulink) and the vehicle-driver system (modelled with MSC.Adams) several tests have been performed on the full model, to assess its behaviour under different conditions like set point following and disturbance rejection, considering both a passive and an active driver. As far as the influence of the driver on the vehicle's dynamics is concerned, the paper shows that it is possible to detect the dynamic forces exerted by the driver on the vehicle. According to these signals, control strategies to switch the vehicle in safe mode can be implemented. In the paper, some issues related to safety have been highlighted.

Keywords*: control design, co-simulation, dynamic model, self-balancing vehicle.

I. INTRODUCTION

The first example of a self balanced two wheels vehicle has been developed, almost for fun, in Lausanne by the members of the team "Industrial Electronics Laboratory" 1 and 2. It was based on the idea that could be possible to realize a mobile, autonomous, inverted pendulum. A small scale prototype was designed and built, showing the feasibility of the idea. Since then other groups have proposed different prototypes, alternate control strategies and uses.

Nowadays several models of two wheeled vehicles are sold both as "toys", or for people "green" transportation in urban environment 3.

Self-balanced two (coaxial) wheeled vehicles can be very useful for several reasons: they can have larger wheels than 4 wheeled carts and therefore can work in a more rugged environment with less energy losses and more comfort, they are more agile since they can rotate in place without the need of a complex 4 wheels steering mechanism. They can be used as a vehicle, driven by a person, can be adapted as a two wheeled wheelchair 4 or as an autonomous robot dedicated to transportation of a payload 5. These vehicles present also safety issues as can be seen in 6, 7, but only a few works analyse control strategies devoted to avoid dangerous situation 8. Several approaches have been adopted to write the equation of motion: Lagrangian 9 10, dynamic equilibrium 1. Several simplifications are in general introduced, mainly when the developing of a control system is of concern: small oscillation in vertical plane, no coupling between longitudinal motion and turn, planar model for the longitudinal motion, ideal contact between (rigid) wheels and ground 2. Only few works deal with the interaction of humans with the vehicle and human body models are quite simplified 11 12. In this work we developed a realistic model of a vehicle (sensors and actuators included), which is under construction in our lab, and of the driver through a 3D Multibody approach, in order to simulate a realistic working condition for the vehicle. Only for the controller synthesis, we used a simpler 2 dof linearized model. The behaviour of the control system has then ben tested with the complete model.

II. VEHICLE CONFIGURATION

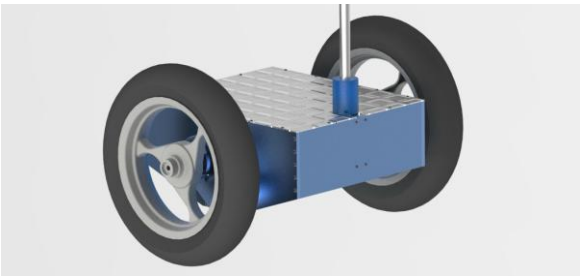

Fig. 1.Vehicle chassis and wheels with tires.

Fig. 1 shows the 3D CAD model of the vehicle. Several parts compose the vehicle:

Manuscript published on November 30, 2019.
* Correspondence Author
Paolo Righettini*, department of Engineering and Applied Sciences, University of Bergamo, Italy. Email: paolo.righettini@unibg.it
Vittorio Lorenzi, department of Engineering and Applied Sciences, University of Bergamo, Italy. Email: vittorio.lorenzi@unibg.it
Bruno Zappa, department of Engineering and Applied Sciences, University of Bergamo, Italy. Email: bruno.zappa@unibg.it
Roberto Strada, department of Engineering and Applied Sciences, University of Bergamo, Italy. Email: roberto.strada@unibg.it

the chassis, the two DC electric motors with planetary gearboxes, the timing belts connecting the drive shafts with the wheels, providing a further speed reduction, wheels and tires. Fig. 2 shows the internal configuration of the system. In particular, the location inside the vehicle's base of the motors, gearboxes, belt transmissions and batteries are highlighted.

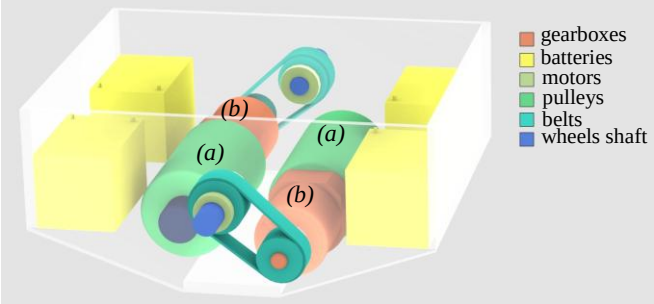

Fig. 2. Internal layout of the chassis with motors (a), gearboxes (b), belts and accumulators. Control electronics not relevant for multibody modelling.

Motors are *Siboni 75PX mod. B14 PAM80*; gearboxes are *Apex mod. PEII090-010.*
Table I summarizes motor/transmission characteristics.

Table I: Motor/transmission characteristics

Motor's rated power [W]	W_m	780
Motor's rated torque [Nm]	C_m	6.8
Motor's rated speed [rpm]	n_m	2050
Gearbox's reduction rate	τ_g	10
Belt transmission reduction rate	τ_b	1.18

Four sensors are used in the vehicle to monitor the state of the system: rotors' angle, inclination and angular speed of the chassis: encoder on motors' shaft providing wheel rotation and also an inertial platform placed on the handlebar of the chassis. It's a MEMS (MPU-6050 of InvenSense) combining a triaxial gyroscope with a triaxial accelerometer.

III. VEHICLE MODEL

The dynamic model of the vehicle has been built using MSC.Adams.
Tires modelling has been widely discussed by Pacejka 13, 14, 15; in this paper, tires have been modelled using the 5.2.1 Model 16, because of its simplicity and small set of parameters since simulation are performed on flat ground, combined effects are negligible and camber angle is absent. Main parameters are tire vertical stiffness k_z (slightly increasing for small deformations), vertical damping c_z and longitudinal friction μ as a function of tire slip speed v_{sx}.
Fig. 3 summarizes the tire slip quantities.

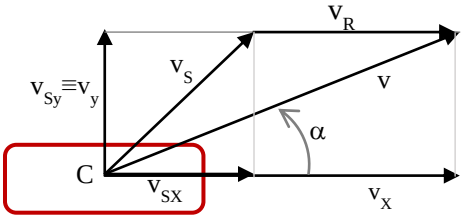

Fig. 3. Definition of tire slip quantities 16

According to model 5.2.1, longitudinal force F_x and lateral force F_y are expressed by the following equations:

$$F_x = \mu \cdot F_z \quad (1)$$

$$F_y = -\left(\mu_{stat} \cdot F_z \cdot \left(1 - e^{-k_\alpha |\alpha|}\right) sign(\alpha)\right) \quad (2)$$

where F_z depends on tire deformation d and deformation speed v_z:

$$F_z = F_{stiff} - F_{damp} \quad (3)$$

$$F_{stiff} = k_z \cdot d^\theta \quad (4)$$

$$F_{damp} = c_z \cdot v_z \quad (5)$$

Tire slip speed v_{sx} depends on wheel's longitudinal speed v_x and on wheel's rolling speed ΩR_1:

$$v_{sx} = v_x - \Omega R_1 \quad (6)$$

Friction coefficient μ depends on tire slip speed, according to diagram represented in Fig. 4.
Rolling resistance moment M_y is calculated from:

$$M_y = f_v F_z R_1 \quad (7)$$

Table II summarizes the tire parameters, while Fig. 4 shows how the friction coefficient is related to the local slip velocity.

Table II: Tire parameters

Vertical_stiffness [N/mm]	k_z	206
Vertical stiffness exponent	θ	1.1
Vertical damping [Ns/mm]	c_z	2.06
Lateral stiffness [N/mm]	k_y	50
Cornering stiffness coefficient [N/deg]	k_α	50
Static friction coefficient	μ_s	0.95
Dynamic friction coefficient	μ_d	0.75
μ_{static} velocity [mm/s]	$v_{\mu s}$	3000
$\mu_{dynamic}$ velocity [mm/s]	$v_{\mu d}$	6000
Rolling resistance coefficient	f_v	0.01

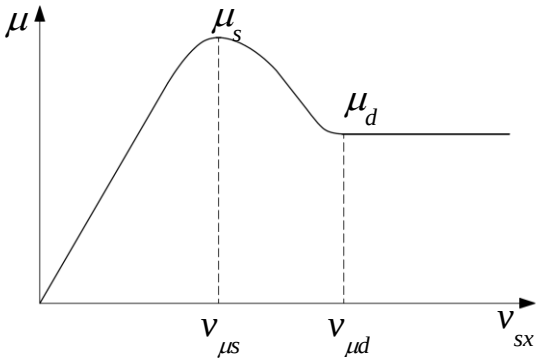

Fig. 4.Friction coefficient vs. local slip velocity 16

Tire parameters have been introduced into the virtual test bench 17 to obtain the diagrams of the relevant characteristics.
Motors have been modelled as massive rotors revolving with respect to the stator (fixed with the chassis). Between the rotor and the stator, the control torque, as defined by Simulink according to the control strategy described in the following sections, is applied. Hence DC motors are seen as ideal torque generators. The hypothesis is quite correct since the motor are driven by current controlled driver.

Gearboxes are modelled through their kinematic relationship between input and output speed (no detail of the epicycloidal mechanism is present), as well as timing belt are kinematically simulated. Both are modelled using the coupler joint present in Adams that imposes a relationship between angular speeds ω_1 and ω_2 of the joints involved:

$$a \cdot \omega_1 + b \cdot \omega_2 = 0 \quad (8)$$

where the ratio *a/b* is the transmission ratio between the two joints. Obviously, input and output torques follow a reciprocal relationship and appropriate reaction torques are applied to the system too.
Four Adams sensors are used in the model to monitor the state of the system: rotors' angle and speed, inclination and angular speed of the chassis. These sensors match the sensors that are placed on the real vehicle and the information elaborated by the control system.

IV. DRIVER MODEL

A multibody model of the driver body has been built too in order to allow the simulation of the typical movements that are required to accelerate/brake or turn a self-balanced vehicle. These manoeuvres are in synthesis a forward/rear leaning (with also crouching for hard braking) and weight shift from one side to the other. In addition, emergency manoeuvres and panic reactions could be reproduced.
More into detail the body model consists of 13 rigid bodies corresponding to feet, calves, thighs, torso+neck+head, arms, forearms and hands. These segments are joined by idealized joints corresponding to the shoulder, elbow, hip, knee and ankle. Hands and feet are properly connected to the vehicle chassis (handlebar and platform respectively). The model dimension and inertial properties are scaled according to the driver height and weight, using the predictive equations proposed in 18, 19 and 20. Table III summarizes the inertial characteristics of the body segments.

Table III: Characteristics of the body segments

Segment	Center mass coordinates [mm]			Mass [kg]	Moments of inertia [kg·mm^2]		
	x	*y*	*z*		J_x	J_y	J_z
Neck	-122	1389	0	1.701	1400	2100	1700
Head	-107	1492	0	3.969	20100	14800	22900
L_Hand	230	1144	-192	0.420	1200	370,84	968,9
L_Forearm	62	1064	-192	1.120	7500	1000	7600
L_UpperArm	-86	1163	-192	1.960	10800	2000	11300
R_UpperArm	-86	1163	192	1.960	10800	2000	11300
R_Forearm	62	1064	192	1.120	7500	1000	7600
L_Thigh	-108	752	-86	7	137600	35000	144400
L_Foot	-64	124	-79	1.015	732,97	4200	4000
L_Calf	-99	401	-80	3.225	51200	5800	52000
R_Foot	-64	124	80	1.015	732	4200	4000
R_Hand	230	1144	192	0.420	1200	370	968
Torso	-126	1163	0	24.85	411700	259900	299000
Pelvis	-122	950	0	9.940	79000	71600	90400
R_Calf	-99	401	80	3.225	51200	5800	52000
R_Thigh	-108	752	86	7	137600	35000	144400

In Fig. 5 and Fig. 6 some views of the driver on the chassis, in the reference position, are shown. Icons highlight human body joints. The circular arrows of Fig. 6 show the actuated joints: elbow, hip and knee.

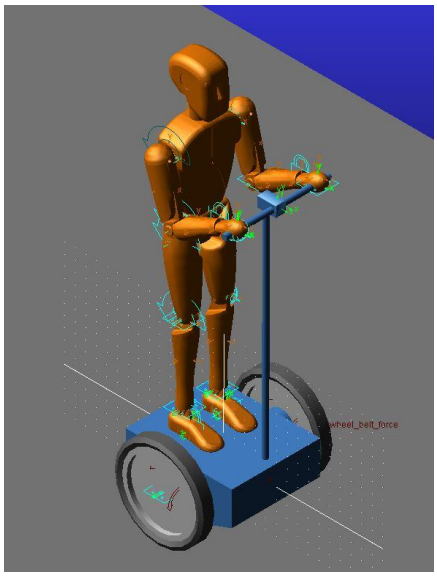

Fig. 5.Driver model

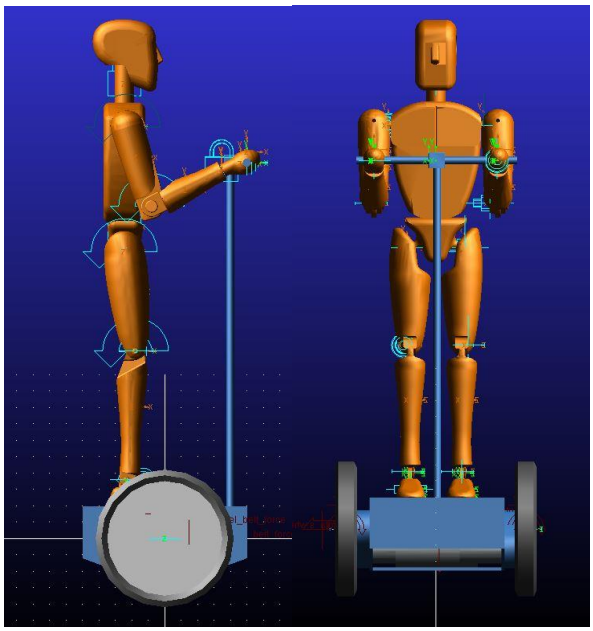

Fig. 6.Driver model (side and front view)

V. LINEARIZED MODEL AND SYNTHESIS OF THE CONTROL SYSTEM

The design of the controller starts from the knowledge of the dynamic model of the vehicle in the longitudinal direction. Fig. 7 shows the scheme of the system and the geometric and mass parameters used to model the system's dynamics. *M* and *J* represent the mass and the mass moment of inertia of the driver and the base of the vehicle as a whole, *R* represents the wheels' radius, *C(t)* the torque applied by the motors to the wheels, φ the rotation of the wheels and θ the rotation of the base.

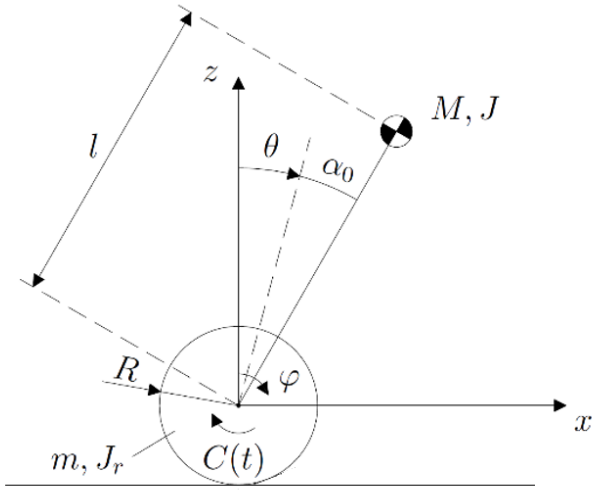

Fig. 7.System's scheme

As far as the driver is concerned, the global mass and moment of inertia have been calculated from average values of segments parameters. In particular, the driver's mass and moment of inertia considered are respectively $M_D = 67\ kg$ and $J_D = 11.70\ kg \cdot m^2$.
Other parameters of the vehicle are summarized in Table IV.

Table IV: Vehicle's parameters

Overall mass [kg]	M	89
Overall moment of inertia [kg·m^2]	J	30.19
Center mass distance from wheels' axis [m]	l	0.71
Wheel's mass [kg]	m	3
Wheel's moment of inertia [kg·m^2]	J_r	0.07
Wheel's radius [m]	R	0.22

According to the Lagrangian approach, the non-linear dynamic model of the system comes from the expressions of the kinetic and potential energies.

$$T = \left(mR^2 + J_r + \frac{1}{2}MR^2\right)\dot{\varphi}^2 + \frac{1}{2}(Ml^2 + J)\dot{\theta}^2 + \\ +MRl(\cos(\theta + \alpha_0))\dot{\varphi} \tag{9}$$

$$U = Mgl\cos(\theta + \alpha_0) \tag{10}$$

Writing Lagrange equations for the two independent coordinates φ and θ, the non-linear dynamic model, expressed as a set of two second-order differential equations, is obtained:

$$\begin{cases} (Ml^2 + J)\ddot{\theta} + MRl(\cos(\theta + \alpha_0))\ddot{\varphi} + \\ -MGl\sin(\theta + \alpha_0) = -C(t) \\ \\ (2MR^2 + 2J_r + MR^2)\ddot{\varphi} + MRl\cos(\theta + \alpha_0)\ddot{\theta} + \\ -\sin(\theta + \alpha_0)\dot{\theta}^2 = C(t) \end{cases} \tag{11}$$

For the synthesis of the controller, linearized equations are needed; the linearization of the equation of motion is made around the equilibrium position defined, in this case, by $\theta = 0$ (the non-linearity of the equations depend only on θ).
The linearized equations of motion in physical coordinates can be obtained using again the Lagrangian approach, taking into account the approximated expression of the energies. These approximated expressions of the energies are the series expansion around the relevant equilibrium position. The series expansion of the kinetic energy is of order zero, while the series expansion of the potential energy is of the second order; (12) and (13) show the series expansion.

$$U(x) = U(x_0) + \nabla U|_{x=x_0}(x - x_0) + \\ \frac{1}{2}(x - x_0)^t\nabla^2 U|_{x=x_0}(x - x_0) \tag{12}$$

$$T(x,\ \dot{x}) = \frac{1}{2}\dot{x}^t M(x_0)\dot{x}\ ,\qquad x = \begin{Bmatrix}\theta \\ \varphi\end{Bmatrix} \tag{13}$$

The linearized equations of motion can be written as:

$$[M]\ddot{x} + [K]x = [Bf]C(t) \tag{14}$$

where

$$[M] = \begin{bmatrix} Ml^2 + J & MRl \\ MRl & 2mR^2 + 2J_r + MR^2 \end{bmatrix} \tag{15}$$

$$[K] = \begin{bmatrix} -Mgl & 0 \\ 0 & 0 \end{bmatrix},\ [B_f] = \begin{bmatrix} -1 \\ +1 \end{bmatrix} \tag{16}$$

In state variables, the equations can be written as follows:

$$\dot{z} = \begin{bmatrix} [0] & [\mathrm{I}] \\ -[M]^{-1}[K] & [0] \end{bmatrix} z + \begin{bmatrix} [0] \\ [B_f] \end{bmatrix} C(t) \tag{17}$$

where

$$z = \begin{Bmatrix} x \\ \dot{x} \end{Bmatrix} = \begin{Bmatrix} \theta \\ \varphi \\ \dot{\theta} \\ \dot{\varphi} \end{Bmatrix} \tag{18}$$

Hence the system dynamics is represented by two physical coordinates or four state variable coordinates. The linearized system is unstable for the presence of poles in the right side of the complex plane. The system satisfies the requirement of controllability and, considering a state feedback scheme, the condition of reachability. It also can be represented in the general form of state equations

$$\begin{cases} \dot{z} = [A]z + [B]C(t) \\ y = [C]z + [D]C(t) \end{cases} \tag{19}$$

where $[C]$ is the identity matrix and $[D]$ is the null matrix.
The controller synthesis proposed is the pole placement method 21 using state feedback. This methodology requires that the input command, the motors' torque in this case, depends on a linear combination of the state

$$C(t) = -[G]z \tag{20}$$

where [G] is a gain matrix with one row and four columns for a total of four controller parameters. Two of them multiplies the system coordinates with derivatives respect to time of order zero, while the others of the first order. Two distinct sub gain matrices can collect the controller gains as a function of the type of coordinates derivatives that multiply.

$$C(t) = -\left[[G_p][G_s]\right]z = -[G_p]x - [G_s]\dot{x} \tag{21}$$

Therefore, the following state-space equation represents the dynamics of the closed-loop system:

$$\begin{cases} \dot{z} = \begin{bmatrix} [0] & [I] \\ -[M]^{-1}[K] - [G_p][B_f] & -[G_v][B_f] \end{bmatrix} z = A_c z \\ y = [C]z \end{cases} \quad (22)$$

The eigenvalues of the A_c matrix define the closed-loop performance of the system; they are a function of the four controller gains, and therefore these gains define the closed-loop response of the system.
The reported results refer to gains obtained fixing the four poles:

$$p_{1,2} = -5 \pm 1.02\, i$$
$$p_{3,4} = -10 \pm 2.03\, i$$

that gives the gains

$$[G] = [-6423 \quad -709 \quad -2215 \quad -409]$$

The closed-loop system, described in physical coordinates, represented by the vector X, as expected, has the two natural frequencies:

$$\omega_1 = 10.2 \frac{rad}{s} \qquad \omega_2 = 5.1 \frac{rad}{s}$$

and the following modes.

$$X^{(1)} = \begin{Bmatrix} -0.2047 \\ 1 \end{Bmatrix} \qquad X^{(2)} = \begin{Bmatrix} -0.1145 \\ 1 \end{Bmatrix}$$

where: $X = \begin{Bmatrix} \theta \\ \varphi \end{Bmatrix}$.

It can be noted that the rotation of the vehicle's chassis is at least 1/5 less than the rotation of the wheels. This condition gives, as a result, reasonable control of the vertical stability of the vehicle with a limited oscillation of the vehicle's base, on which the driver is placed.

VI. SIMULATIONS AND RESULTS

The simulations have been carried out by means of a co-simulation technique between Matlab-Simulink and MSC.Adams as schematically shown in Fig. 8, where $C(t)$ are the motor torques applied to the wheels, z is the vehicle state variables vector and X_D is the coordinates vector of the driver. The comprehensive system equation implemented in MSC.Adams can be summarized as follows:

$$\begin{cases} [M]\{\ddot{q}\} + \left[\Psi_q\right]^T \{\lambda\} = \{F_e\} \\ \{\Psi\} = 0 \end{cases} \quad (23)$$

where:

- $[M]$ is the mass matrix
- $\{q\}$ is the coordinate vector
- $\{\Psi\}$ is the constraint equations vector
- $\left[\Psi_q\right]$ is the Jacobian matrix
- $\{\lambda\}$ is the Lagrange multipliers vector
- $\{F_e\}$ is the generalized forces vector

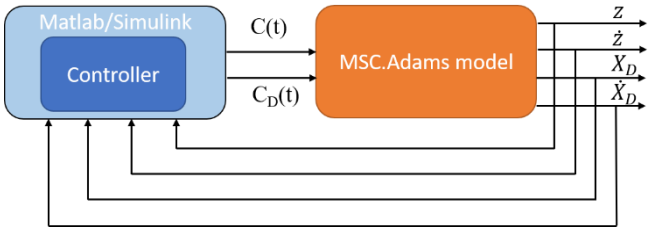

Fig. 8.Co-simulation scheme

Using the model developed, several simulations have been carried out for different conditions. In particular, the simulations can be divided in the categories summarized in Table V:

Table V: Simulations categories

Category	*Motion*	*Set-point*	*Driver*
A	longitudinal plane	Externally assigned	Still
B	longitudinal plane	Externally assigned	Moving
C	longitudinal plane	Assigned by driver	Moving
D	longitudinal plane	Assigned by driver	Moving

A. Motion set-point assigned and driver standing still

This kind of simulations is performed giving a motion set-point profile to the vehicle, considering the driver as a rigid body fixed to the chassis. Fig. 9 and Fig. 10 show the results for a simulation in which a 1.8 m/s steady state velocity set-point has been assigned. In particular, Fig. 9 shows the set-point (red line) and the followed velocity (blue line); Fig. 10 represents the behavior of the chassis angle.

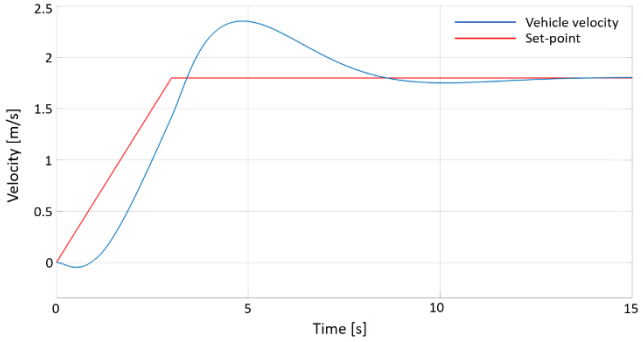

Fig. 9.Set-point and followed velocity

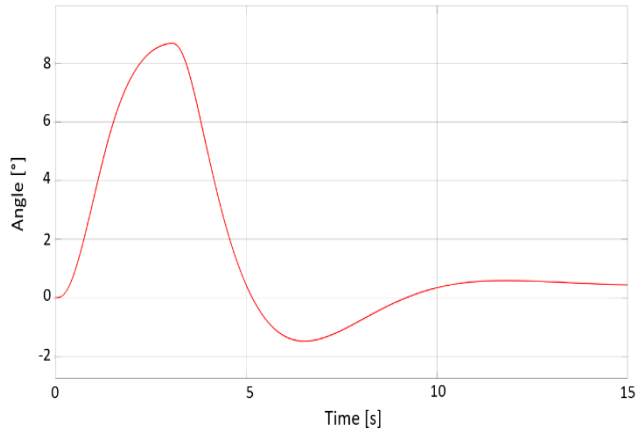

Fig. 10. Chassis incline angle

B. Motion set-point assigned and moving driver

In this case, the simulation's target is to show how the movements of the driver influence the vehicle's dynamics. Fig. 11 shows the movements of the driver: knee (violet), elbow (blue), hip (orange) and shoulder (green). Fig. 12 shows the consequent change of the center of mass position.

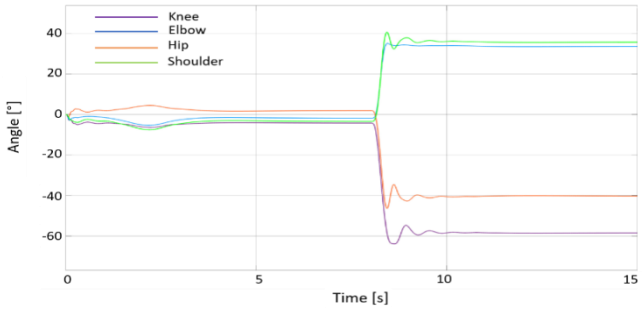

Fig. 11. Driver's movements

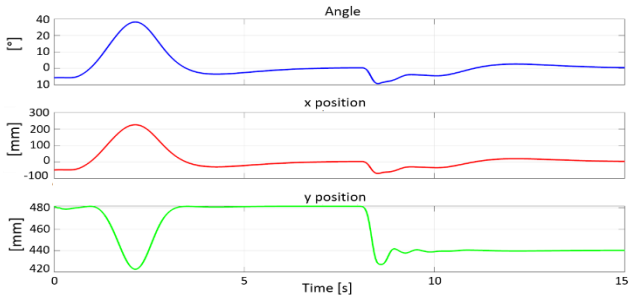

Fig. 12. Driver's center of mass coordinates

The driver's movements also influence both the chassis' forces and the wheels' torques. Fig. 13 and Fig. 14 show that both of them varies according to the driver's movements.

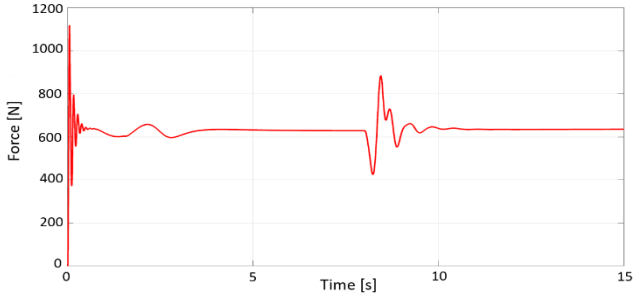

Fig. 13. Force on the chassis platform

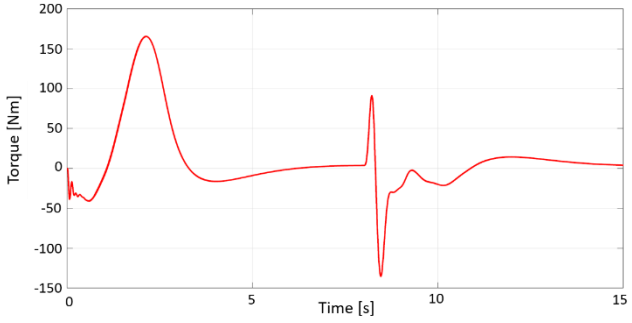

Fig. 14. Wheels' torque

C. Motion set-point assigned by the driver movement

In this simulation, the motion profile set-point is based on the driver's movements. Fig. 15 shows the results of a simulation in which the driver generates the set-point represented using a red line, while the law of motion followed by the vehicle is the blue one. In this case the acceleration motion set-points depends on pitch angle of the chassis.

Fig. 16 and Fig. 17 represent respectively the consequent chassis' pitch angle and driver's center of mass position.

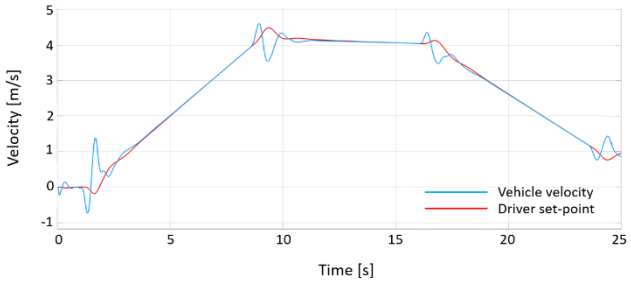

Fig. 15. Set-point generated by the driver

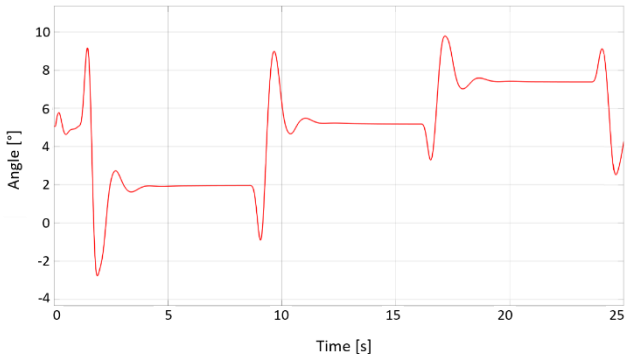

Fig. 16. Chassis pitch angle

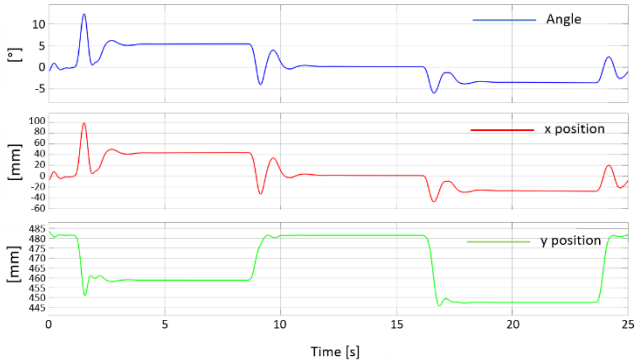

Fig. 17. Center of mass position

D. Simulations for safety

Safety is a critical topic concerning the use of a self-balanced vehicle. These simulations aim to show that it is possible to detect signals from the vehicle that can be used to identify emergency conditions, on whose bases the vehicle must switch in safety mode.

As an example, Fig. 18 shows that if, during the simulation, the force exerted on the chassis by the driver increases more than a threshold value (in this case 150 N), the system enter a safety state in which an emergency braking in order to stop the vehicle is applied, as shown in Fig. 19.

The increase of force could be a consequence of a "panic behavior" of the driver like shownin Fig. 20 where at simulation time 12 s. The driver suddenly lowers, as shown by the y position of the center of mass in Fig. 20, generating the force increment that makes the vehicle enter the emergency braking state.
Besides, in order to guarantee a safe emergency braking, the chassis incline cannot be too high; Fig. 21 shows the results of a simulation in which the incline does not overcome 20°.

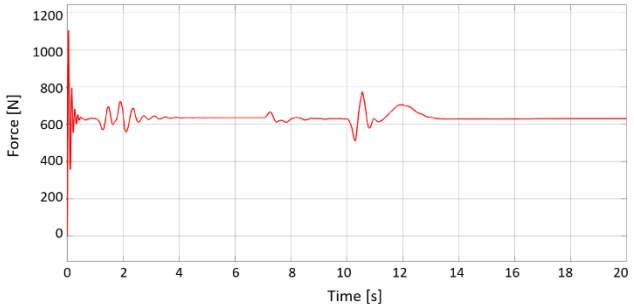

Fig. 18. Force on the chassis platform

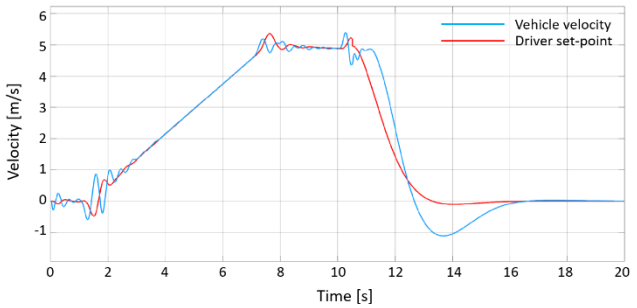

Fig. 19. Driver set-point and vehicle's speed.

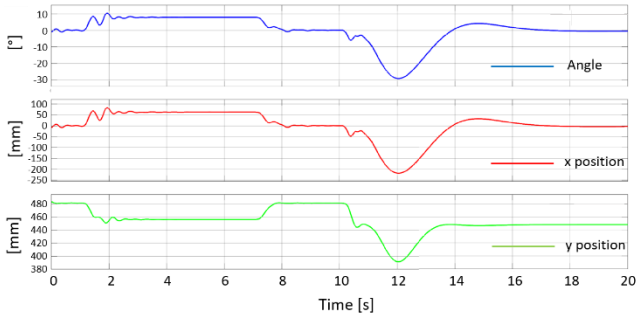

Fig. 20. Center of mass position

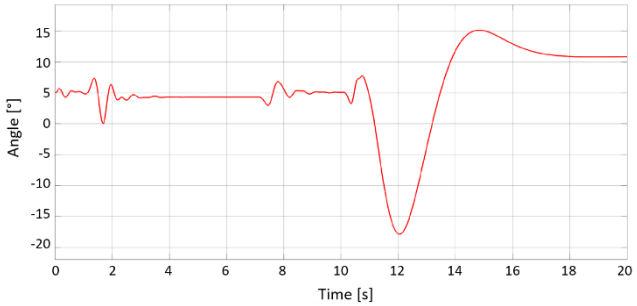

Fig. 21. Chassis' pitch angle

VII. CONCLUSIONS

The paper presents a comprehensive dynamic model of a self-balanced vehicle which includes a detailed physical description of the interaction between the wheels and any type of ground. Moreover, the proposed model takes into account also the dynamic behavior of the motor/transmission system. The model of the vehicle is coupled with a proper description of the driver dynamics using several segments with 3 actuated joints. Both of them have been developed in MSC.Adams;the overall 3D model allows to take into account also the coupling between longitudinal motion and turn. The interactions between the two models allow to evaluate the force exerted between the vehicle and the driver. The control system, implemented in Matlab-Simulink environment, allows both to control the stability of the vehicle and to actuate the three driver joints to achieve the proper configuration for the simulations of any type of movements.
The analyses of the human-vehicle interaction have been developed using Matlab-Simulink-MSC.Adams co-simulations. Several analyses have been carried out, showing that the proposed approach gives the possibility to simulate several conditions, allowing to investigate both the behavior of the vehicle alone, assuming the driver as a rigid body fixed to it, and the influence of the driver's movements on the dynamics of the vehicle itself.
The latter result opens a way towards the safety management of the vehicle; the simulations clearly show that it is possible to identify some emergency running conditions and consequently to make the vehicle enter in a safe state where, for example, an emergency braking could be acted.
In conclusion, the model developed seems to be a powerful tool to investigate in deep several vehicle/driver/control running conditions.

REFERENCES

1. A. D'Arrigo, "Veicolo elettrico sperimentale a due ruote parallele coassiali indipendenti," Thesi di laurea, EPFL/Politecnico di Milano, Lausanne, Switzerland/Milan, Italy, 1997
2. F. Grasser, A. D'Arrigo, S: Colombi and A.C. Rufer "JOE: A Mobile, Inverted Pendulum" IEEE TRANSACTIONS ON INDUSTRIAL ELECTRONICS, VOL. 49, NO. 1, FEBRUARY 2002, pp. 107-114
3. Kamen Dean, Segway, http://www.segway.com, 2001
4. J. Huang, F. Ding, T. Fukuda, T. Matsuno, "Modelling and velocity control of a novel narrow vehicle based on mobile inverted pendulum". IEEE Trans Control Syst Technol. 2013;21(5):1607–17
5. S. R. Larimi, P. Zarafshan, S. Ali A. Moosavian, "A New Stabilization Algorithm for a Two-Wheeled Mobile Robot Aided by Reaction Wheel", Journal of Dynamic Systems, Measurement, and Control, JANUARY 2015, Vol. 137, pp. 011009-1 011009-8
6. J. Xua, , S. Shanga, G. Yud, H. Qie, Y. Wangd. and S. Xu" Are electric self-balancing scooters safe in vehicle crash accidents?" Accident Analysis and Prevention 87 (2016) 102–116 (Elsevier)
7. J. Ashurst, B. Wagner, "Injuries Following Segway Personal Transporter Accidents: Case Report and Review of the Literature", Western Journal of Emergency Medicine: Integrating Emergency Care with Population Health, Volume XVI, no. 5 : September 2015, pp. 693-695
8. N. Ding, M. Shino, N. Tomokuni, G. Murata, "Fall Avoidance Control of Wheeled Inverted Pendulum Type Robotic Wheelchair While Climbing Stairs" International Journal of Biomedical and Biological Engineering Vol:11, No:4, 2017, World Academy of Science, Engineering and Technology,

9. A. M Almeshal, K. M Goher, and M. O Tokhi,.. "Dynamic modelling and stabilization of a new configuration of two wheeled machines". Robotics and Autonomous Systems, 61(5), 443–472(2013).
10. S. Haddout "Nonlinear reduced dynamics modelling and simulation of two-wheeled self-balancing mobile robot: SEGWAY system", Systems Science & Control Engineering, 6:1, 1-11(2018)
11. S. Jeong, K. Kouzai and S. Noguchi "On the braking behavior of a self-balancing personal mobility vehicle", Advanced Robotics, 30:7, 449-458.
12. M. CIĘŻKOWSKI "Modelling the interaction between two-wheeled self-balancing vehicle and its rider", Int. J. of Applied Mechanics and Engineering, 2013, vol.18, No.2, pp.341-351 DOI: 10.2478/
13. H.B Pacejka, E. Bakker, and L. Lidner, "A New Tire Model with an Application in Vehicle Dynamics Studies", SAE paper 890087, 1989.
14. H.B Pacejka and E. Bakker, "The Magic Formula Tyre Model", Proceedings of the 1st International Colloquium on Tyre Models for Vehicle Dynamics Analysis, Swets & Zeitlinger B.V., Amsterdam/Lisse, 1993.
15. H.B. Pacejka, "Tyre and Vehicle Dynamics", Butterworth-Heinemann, 2002.
16. https://www.mscsoftware.com/product/adams
17. V. Lorenzi, B. Zappa, P. Righettini, R. Strada "Teaching tyre testing and modelling to undergraduate Mechanical engineering students", in proceedings of the 12th International Technology, Education and Development Conference, Valencia, 2018.
18. McConville, J.T., Churchill, T.D., Kaleps, I., Clauser, C.E., Cuzzi, J., 1980. Anthropometric relationships of body and body segment moments of inertia. Technical Report AFAMRL-TR-80-119, Aerospace Medical Research Laboratory, Wright–Patterson Air Force Base, Dayton, Ohio.
19. B.Zappa, F.Casolo, G.Legnani "Analysis and synthesis of 3D motion for multi-body systems with regard to sport performances. IX World Congress on the Theory of Machines and Mechanisms, Milano, Settembre 1995.
20. R. Dumas, L. Che`ze, J.-P. Verriest, "Adjustments to McConville et al. and Young et al. body segment inertial parameters", Journal of Biomechanics 40 (2007) 543–553
21. Kautsky, J., N.K. Nichols, and P. Van Dooren, "Robust Pole Assignment in Linear State Feedback," International Journal of Control, 41 (1985), 1129-1155

AUTHORS PROFILE

Paolo Righettini was born in Salò, Italy, in 1966. He received the Master degree in Mechanical Engineer in 1991 from Politecnico di Milano. In 1994 he became Asisistant Professor of Applied Mechanics at Politecnico di Milano. In 2000 he became Associate professor at Politecnico di Milano; subsequently, he moved to the Università degli Studi di Bergamo where, since 2007 he has been Associate Professor at the School of Engineering. Here he is the head of the mechatronic research group and head of the Mechatronics and Mechanical Systems Dynamics laboratory. His research activities mainly concern the dynamic modelling and the control of mechatronic systems, kinematic and dynamic synthesis of robotic devices, kinematic synthesis and dynamic control of parallel kinematic robots. In these contest, he has interest in the modelling and control of electrical, hydraulic and piezoelectrical actuating systems. The research activities regard both the theoretical/numerical part and the experimental one.

Vittorio Lorenzi was born in Bergamo, Italy, in 1962. He received the Master degree in Mechanical Engineer in 1987 from Politecnico di Milano. In 1992 he got his PhD in Applied Mechanics and became Assistant Professor at Politecnico di Milano. Since 2001 he has been Associate Professor at School of Engineering of the Università degli Studi di Bergamo. He teaches courses on Multibody Systems Dynamics, Vehicle Dynamics and Safety and Mechanics of Machines. In Politecnico di Milano we was involved in researches about sport biomechanics, hip and dental implantology and hand and wrist biomechanics. His actual main research activity is dedicated to Multibody Systems Dynamics.

Bruno Zappa was born in Tirano, Italy, in 1962. He received the Master degree in Mechanical Engineer at Politecnico di Milano in 1991 and in 1996 he got his PhD in Applied Mechanics. From November 1999 to October 2002 he was assistant professor at the University of Bergamo. Since November 2002 he has been Associate Professor at School of Engineering of the same University. At present he teaches courses on Mechanics of robots, Drives for Mechanical Systems and Mechanics of Machines. His research interests have covered both sport and rehabilitation biomechanics with particular regard to the study of devices for the assessment of dynamic inputs to the vestibula, and for the analysis of human motion. Several researches have been conducted in the field of automatic machinery analysis and design and on the dynamic of 3D free-flying space manipulators. His current research interests include robotics, mechatronics, kinematics and dynamics of multibody systems.

Roberto Strada was Born in Vimercate, Italy, in 1969. He received the Master degree in Mechanical Engineering at Politecnico di Milano in 1994. In 2001 he got the PhD degree in Applied Mechanics at Politecnico di Milano. Since 2002 he has been Assistant Professor of Applied Mechanics at the School of Engineering of the Università degli Studi di Bergamo. His research activities mainly concern the dynamic modelling and simulation of driving systems for Mechatronics; in particular, the activity deals with the study of the dynamic characteristics of systems and components driven by hydraulic actuators, pneumatic actuators and electric actuators. Besides theoretical and numerical analysis, experimental activities have been performed. Results of the research activities have been published in international journals and presented at international conferences.